

Quasielastic proton-nucleus scattering at 300–800 MeV

H. Esbensen

Physics Division, Argonne National Laboratory, Argonne, Illinois 60439

G. F. Bertsch

Cyclotron Laboratory and Department of Physics and Astronomy, Michigan State University, East Lansing, Michigan 48824

(Received 7 April 1986)

Surface response model results for quasielastic nucleon-nucleus scattering are compared to recent intermediate energy (p,p') spectra. The energy and target dependences of the quasielastic peak, as well as the dependence on momentum transfer, are quite accurately described by this model. Discrepancies at large energy and momentum transfers are ascribed to multistep processes, and they become more significant at lower beam energies. Shell structures of finite nuclei, which are not contained in the model, are the main source of the discrepancies at small momentum transfers.

I. INTRODUCTION

Inclusive spectra for quasielastic proton scattering on heavy nuclei are now available over a wide range of beam energies. Recent data¹ cover the energy range of 300–500 MeV, which has not previously been studied in a systematic way. Quasielastic proton scattering at 800 MeV (Refs. 2 and 3) is quite well described by single scattering in the surface response model.^{4,5} The (p,n) charge exchange reactions at 200 MeV (Ref. 6) are also fitted by single scattering in the distorted wave impulse approximation.⁷ At lower energies the quasielastic peak becomes less pronounced and tends to disappear.^{8,9} Below 100 MeV the inclusive proton spectra have been fitted in a model based on single and double scattering plus proton evaporation from the compound nucleus.¹⁰

The new data at 300–500 MeV cover an energy regime where single scattering should dominate the quasielastic peak. The purpose of the present paper is to investigate this in detail, making use of the surface response model. Our model is based on the surface response of semiinfinite nuclear matter, the free nucleon-nucleon (NN) elastic scattering amplitude, and Glauber theory. The model can be derived from the distorted wave impulse approximation (DWIA) at high beam energies. When the energy is large, the projectile wave function approaches the eikonal limit and the absorption, as determined by the imaginary part of the optical potential, becomes similar to that obtained in Glauber theory. However, in typical applications of the DWIA at intermediate energies, the absorption is much less from optical treatments than expected on the basis of the target density and the free nucleon-nucleon cross section.

This has led to much debate in recent years about the magnitude of the mean free path in nuclear matter. The discussion has mainly concerned the parametrization of the local optical potential for elastic nucleon-nucleus scattering,¹¹ and the mean free path that one can extract from the associated reaction cross section^{11–13} (which has not directly been measured). A further complication of the subject is the importance of the nonlocality of the op-

tical potential.^{14,15} Although this discussion has mainly concerned beam energies that are smaller than those we consider in the present article, it is anyhow interesting to study the quasielastic peak in detail at 300–500 MeV and to see how well the Glauber theory can account for the absolute magnitude and the target dependence.

We remind the reader of the surface response model in Sec. II. There we also estimate the reduction of the total nucleon-nucleon cross section due to Pauli blocking and residual interactions in the surface response. The comparisons to measured (p,p') spectra are presented in Sec. III, and Sec. IV contains our conclusions.

II. SURFACE RESPONSE MODEL

In the surface response model^{4,5} the double differential cross section for inelastic proton-nucleus scattering is given by the factorized formula:

$$\frac{d^2\sigma}{d\Omega d\omega} = N_{\text{eff}} \sum_{T,S} \left[\frac{d\sigma_{\text{NN}}}{d\Omega} \right]_{T,S} S_{T,S}(q,\omega). \quad (1)$$

The three factors in this formula are explained in the following. The effective number of target nucleons, N_{eff} , is determined by Glauber theory for single scattering,

$$N_{\text{eff}} = \int d^2\mathbf{b} n(b) \exp[-n(b)\sigma_{\text{NN}}], \quad (2)$$

where σ_{NN} is the total NN cross section and

$$n(b) = \int_{-\infty}^{\infty} dx \rho_A [(x^2 + b^2)^{1/2}] \quad (3)$$

is the number of target nucleons per fm² along a straight line trajectory at an impact parameter b with respect to the center of the target nucleus. The straight line trajectory approximation makes the model most reliable at small scattering angles. The target density ρ_A is obtained from the parametrizations of measured charge densities given in Ref. 16.

The formula furthermore contains the elastic NN cross section, $(d\sigma_{\text{NN}}/d\Omega)_{T,S}$, decomposed into contributions from the different spin-isospin channels (S,T) of target excitations. These contributions are calculated from the

free NN scattering amplitude and the phase shifts given in Ref. 17, supplied with one-pion exchange phase shifts at higher partial waves.

Finally, the surface response functions $S_{T,S}(q,\omega)$, which are functions of the momentum transfer q and the excitation energy ω , are obtained from the Green's function (or polarization operator) for semiinfinite nuclear matter.⁵ The separable residual interactions discussed in Ref. 5 are used to calculate the response in the different spin-isospin channels in the random phase approximation (RPA). The surface response is generated by a field $F(z)\exp(i\mathbf{q}\cdot\mathbf{r})$ that is consistent with Glauber theory. The construction of this field is discussed in detail in Ref. 18, Sec. IIB, and the total response is normalized to unity if we neglect the residual interaction and the effect of Pauli blocking.

The response functions have a weak dependence on the target and the beam energy via the field $F(z)$, but one can ignore this dependence in the qualitative arguments that will be given later on. The target dependence in Eq. (1) is mainly contained in the factor N_{eff} , whereas the energy dependence is contained in the elastic NN cross sections, and in N_{eff} through the total NN cross section.

A. Pauli blocking

The value of the total NN cross section σ_{NN} that enters into the Glauber calculation has usually been taken from free scattering. This is a reasonable approximation at high energies, but there are important medium corrections at lower energies. These corrections are in general difficult to calculate. The medium corrections to the free t matrix, which are treated in Brueckner theory, are beyond the scope of the present study. Some of the effects associated with the RPA surface response can be estimated, namely the Pauli blocking and the residual particle-hole interactions. Below pion threshold the effective value would then be

$$\sigma_{\text{NN}}^{\text{eff}} = \int_{4\pi} d\Omega \int_0^\infty d\omega \sum_{T,S} \frac{1+2T}{2} \left[\frac{d\sigma_{\text{NN}}}{d\Omega} \right]_{T,S} S_{T,S}(q,\omega). \quad (4)$$

Here the factor of $\frac{1}{2}$ takes care of double counting when integrating over 4π , and the factor $(1+2T)$ accounts for all the isospin channels that can attenuate the unscattered proton beam in (p,p') and (p,n) reactions. The NN scattering amplitude is still determined by free scattering.

Equation (4) has to be solved self-consistently, since the surface response is generated by a field $F(z)$ that is consistent with Glauber theory and therefore depends on $\sigma_{\text{NN}}^{\text{eff}}$.¹⁸ The Pauli blocking is important at small momentum transfers and reduces the effective NN cross section compared to the free value. There are both attractive and repulsive residual interactions. The isoscalar interaction is attractive and enhances the surface response at low q , so the total effect of residual interactions may act against the Pauli blocking.

The numerical calculation of Eq. (4) is straightforward but rather time consuming. We shall therefore make some simple estimates. We can get a quick estimate by ignoring the residual interactions and replacing the response

by the Lindhard function of the free Fermi gas response. With our normalization of the response this yields the momentum-dependent Pauli blocking factor

$$P_{\text{FG}} = \int_0^\infty d\omega S(q,\omega) = \frac{y}{2}(3-y^2) \text{ for } y < 1 \\ = 1 \text{ for } y > 1, \quad (5)$$

where $y = q/(2k_F)$ and k_F is the Fermi momentum. If we assume that the free NN scattering is independent of q we obtain the following result in terms of the free scattering cross section σ_{NN} :

$$\sigma_{\text{NN}}^{\text{eff}} = \sigma_{\text{NN}} y_0 \left(1 - \frac{1}{5} y_0^2\right) \text{ for } y_0 < 1 \\ = \sigma_{\text{NN}} \left[1 - \frac{1}{5 y_0^2}\right] \text{ for } y_0 > 1, \quad (6)$$

where $y_0 = \sqrt{T_{\text{lab}}/(4\epsilon_F)}$, T_{lab} is the kinetic energy of the nucleon, and ϵ_F is the Fermi energy. We can thus expect a 20% reduction at an energy that is four times the Fermi energy.

The above estimate is too crude, partly because NN scattering is forward peaked and also because the response is generated at the surface of the nucleus, where the local Fermi energy varies drastically. Both effects can be included in a local Fermi gas approximation, and the average Pauli blocking factor becomes

$$\langle P_{\text{PB}}(q) \rangle = N_{\text{eff}}^{-1} \int d^2\mathbf{b} n(b) \exp[-n(b)\sigma_{\text{NN}}^{\text{eff}}] \\ \times P_{\text{FG}} \left[\frac{q}{2k_F(b)} \right]. \quad (7)$$

Using this expression for the energy-integrated response in Eq. (4) we obtain the result shown in Fig. 1. The absorption cross section in free NN scattering that becomes important above 300 MeV has been added. The reduction of the effective cross section, compared to the value for free scattering, is much larger than predicted by the simple es-

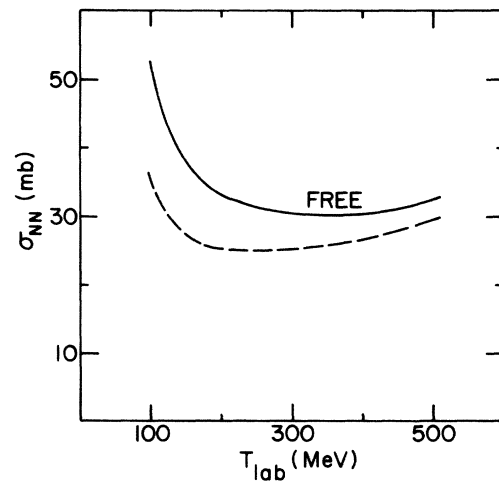


FIG. 1. Total nucleon-nucleon cross sections as functions of the beam energy. The fully drawn curve is for free scattering, and the dashed curve includes the effect of Pauli blocking in the local Fermi gas approximation for the surface response.

time Eq. (6). This is due to the forward peaking of the free NN scattering and the fact that the Pauli blocking factor is smallest at small momentum transfers.

B. Medium corrections

The qualitative features of the surface response functions have been studied in Ref. 5. The total responses for the isospin excitations are shown in Fig. 5 of that reference. The Pauli blocking factor for the free response is quite similar to the one obtained in the local Fermi gas model Eq. (7), except near $q=0$. In fact, they yield about the same σ_{NN}^{eff} . Furthermore, σ_{NN}^{eff} does not change much at 300–500 MeV if one also includes the residual interactions in the different spin-isospin channels. The most important channels at these energies are the isoscalar and the $T=S=1$ channels; the isoscalar response is enhanced, but the $T=S=1$ response is reduced, leaving σ_{NN}^{eff} close to the value obtained from the local Fermi gas model. At higher energies a larger fraction of the NN cross section goes to higher momentum transfers, where neither Pauli blocking nor residual interactions play any role. Moreover, the isoscalar channel starts to dominate NN scattering, so σ_{NN}^{eff} will approach the value for free NN scattering in this limit.

The above discussion of σ_{NN}^{eff} is schematic because we have just argued from the behavior of the total responses without explicitly performing the multidimensional integral implied by Eq. (4). We have also ignored medium corrections to the t matrix which determines the second factor, $d\sigma_{NN}/d\Omega$, in Eq. (1). The conventional way to study this effect is to solve the Bethe-Goldstone equation for the G matrix. The relevant densities for such a calculation would be of the order of and less than half nuclear matter density. At 300 MeV and above these corrections are expected to be small. One of the main corrections is due to the Pauli blocking. One can make a qualitative estimate from the optical theorem which relates the total NN cross section to the imaginary part of the scalar t matrix at $q=0$. Using the cross sections shown in Fig. 1 we find that this component of the t matrix is reduced by the factor $\sigma_{NN}^{\text{eff}}/\sigma_{NN} \cong 0.84$ at $q=0$. We expect a correction factor much closer to one at the large momentum transfers that we shall consider in the next section.

The enhancement of the isoscalar response over the free response is much smaller in the interior of a nucleus because the residual interaction in this channel is much weaker at nuclear matter density. Consequently, an even smaller value of σ_{NN}^{eff} is expected in the nuclear interior than we obtain with the surface response model. However, other effects such as nonlocality complicate the question further and we shall not attempt to estimate these corrections.

III. COMPARISON TO (p,p') SPECTRA

The inclusive (p,p') spectra of Ref. 1 make it possible to test the surface response model in detail with respect to the energy and target dependence and the dependence on momentum transfer. The uncertainty in the data was estimated to be about 15%. For a fixed target and beam energy the relative comparison of the quasielastic peaks at

different scattering angles is more accurate. We display two sets of results with the Glauber calculation based on the total NN cross section for free scattering (fully drawn curves) and based on the effective NN cross section obtained from the local Fermi gas approximation (dashed curves). Medium corrections to the effective NN interaction between the projectile and the target nucleons, which we have ignored, would probably reduce the dashed curves towards the fully drawn curves, the reduction being smallest at the largest momentum transfers. We shall therefore consider the dashed and the fully drawn curves as two extreme estimates of the single scattering cross section.

The proton spectra for reactions on ^{58}Ni are shown in Fig. 2 at an incident energy of 400 MeV and at four different scattering angles, corresponding to momentum transfers of 1.3, 1.6, 2.0, and 2.4 fm^{-1} . The position and the magnitude of the quasielastic peak is fairly well reproduced by the model. The tail of the observed spectra at larger energy losses seems to become more dominant at larger scattering angles, and the model fails to account for this part of the spectra.

The calculated peak height is seen to underpredict the data at the larger scattering angle. This is consistent with the model calculations of Ref. 19, where the contribution from double scattering was estimated. Using that model we estimate that the contribution from double scattering increases the peak height by 15% at the largest scattering angle, and only by 5% at the smallest angle shown in Fig. 2. Let us also mention that the straight line trajectory approximation used in the Glauber calculation may not be accurate at the largest scattering angle.

The target dependence is illustrated in Fig. 3 for 400 MeV (p,p') reactions on ^{12}C and ^{206}Pb , at two scattering angles of 16 and 30 deg. The comparison between the model predictions and the experimental data would be equally good for the two targets if the calculated results for ^{12}C were increased by 20%. The target dependence originates primarily from the Glauber calculation of N_{eff} , whereas the response function, generated at the surface of semiinfinite nuclear matter, is rather insensitive to the target. The model predicts a ratio of 0.31 for the peak heights in ^{12}C and ^{206}Pb , whereas the data show a ratio of about 0.37. Comparing the peak heights in ^{58}Ni and ^{206}Pb , the model predicts a ratio of 0.69. The observed spectra show a ratio of about 0.75.

There seems to be a systematic trend that the model underpredicts the data for the lightest target. However, this trend is not much more significant than the experimental uncertainty of 15%. The scaling property of the model associated with the target dependence is therefore surprisingly good in the present comparison; *a priori* one would expect that the response of ^{12}C would be very different from the surface response of semiinfinite nuclear matter.

The energy dependence of the quasielastic peak is shown in Fig. 4 for (p,p') reactions on lead targets. The data at 800 MeV are from Ref. 3, whereas the data at 300–500 MeV are from Ref. 1. The different scattering angles have been selected to yield about the same momentum transfer: 1.4, 1.6, 1.5, and 1.7 fm^{-1} at 300, 400, 500, and 800 MeV, respectively. The most noticeable feature of this figure is the better agreement at the higher beam

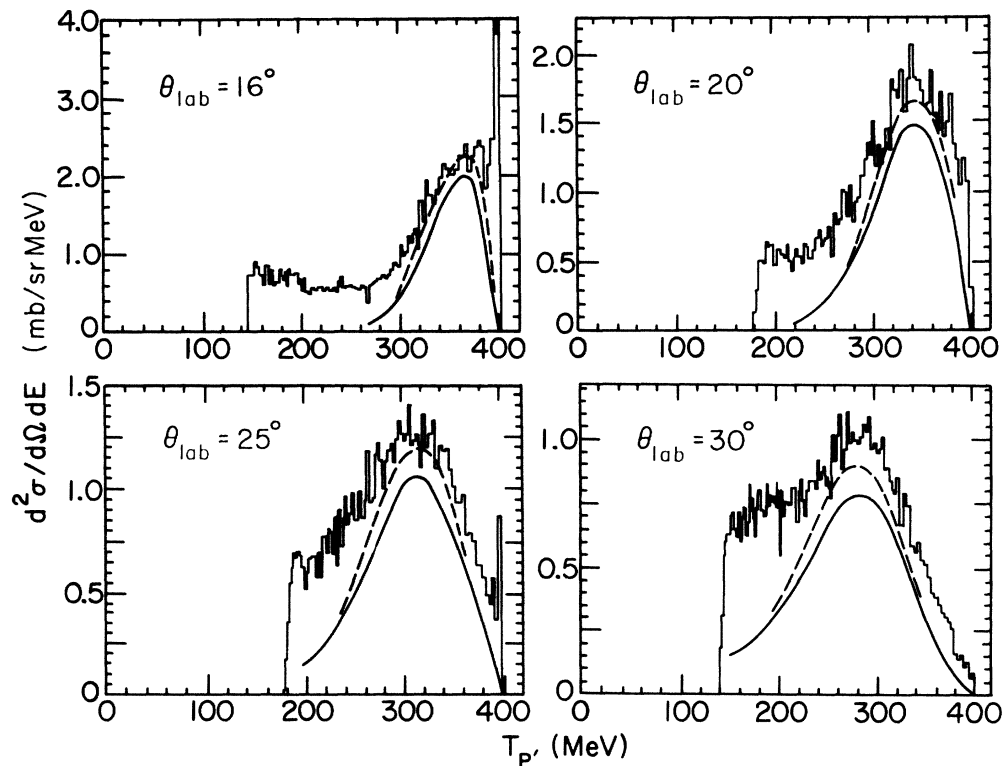


FIG. 2. Energy spectra for 400 MeV (p,p') reactions on ^{58}Ni at four different laboratory scattering angles. The measured spectra (histograms) are from Ref. 1. The calculated results in the surface response model are based on the total nucleon-nucleon cross sections shown in Fig. 1, for free scattering (fully drawn curves) and in the local Fermi gas approximation (dashed curves).

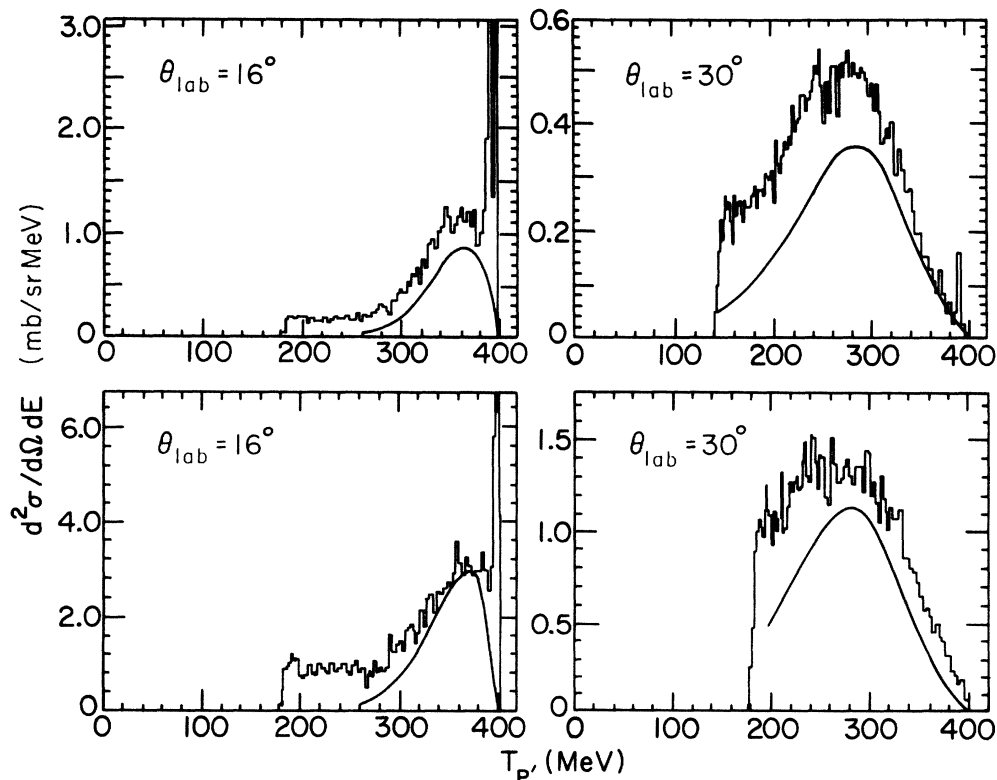


FIG. 3. Energy spectra for 400 MeV (p,p') reactions on ^{12}C (upper figures) and on ^{206}Pb (lower figures), at two different laboratory scattering angles. The measured spectra (histograms) are from Ref. 1. The calculated results in the surface response model are based on the total nucleon-nucleon cross section for free scattering.

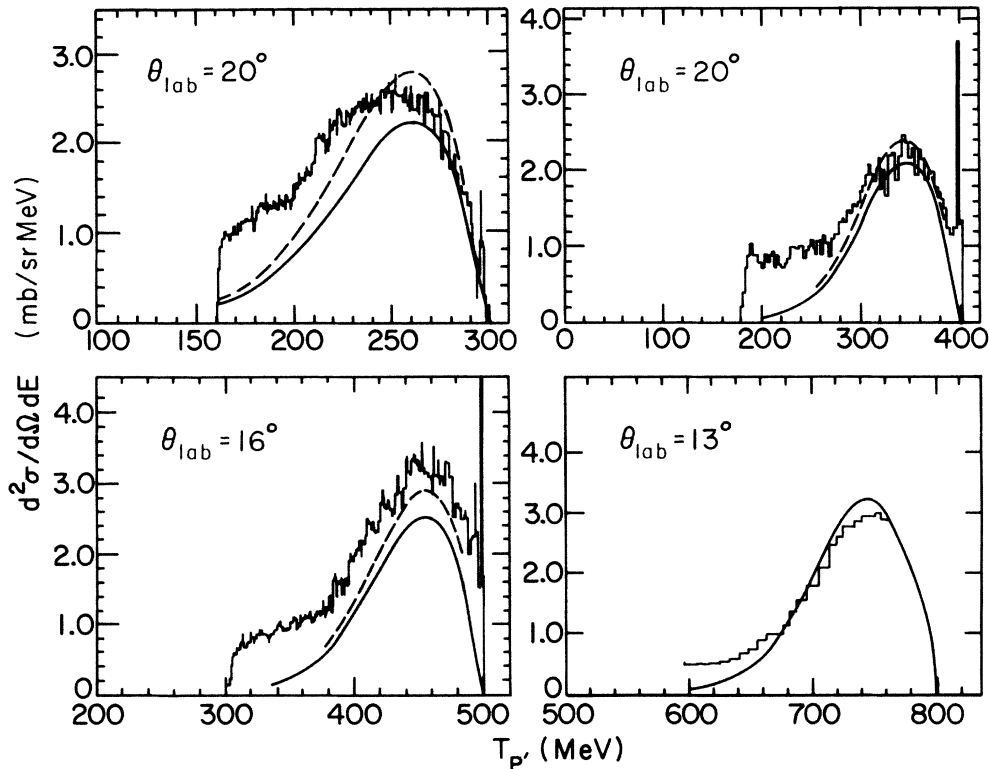


FIG. 4. Energy spectra for (p,p') reactions on lead at four different beam energies and scattering angles. The measured spectra (histograms) are from Ref. 1 (at 300, 400, and 500 MeV) and Ref. 3 (at 800 MeV). The calculated results in the surface response model are based on the total nucleon-nucleon cross section for free scattering (fully drawn curves) and in the local Fermi gas approximation (dashed curves).

energy, in particular at the larger energy losses. There is a simple explanation for this tendency, which can be seen in the folding model for double scattering.¹⁹ There the folding is performed in the space of energy and momentum transfer. The response functions, normalized as discussed in Sec. II, are rather insensitive to the beam energy. The NN scattering cross section is of course energy dependent, and the most significant energy dependence is in the range of permitted momentum transfers. For a given energy loss and momentum transfer the contribution from double scattering will decrease as the beam energy goes up, simply because a smaller fraction of the NN cross section will be located in the region where there is an appreciable response.

Let us finally mention that the effect of the residual interactions in our model is not very important in any of the cases discussed above, with momentum transfers larger than 1 fm^{-1} . If we instead had used the free (noninteracting) response in all channels, the steepness of the energy loss distribution would be smaller at the lower excitations, but the peak heights would only change by a few percent. In contrast, inelastic electron scattering shows a quasielastic peak that is shifted upward in energy from the free response. In Ref. 20, discussing the quasielastic peak in ^{12}C at momentum transfer larger than 1.25 fm^{-1} , the persistent interaction effects are treated by using an effective mass $m^* = 0.82m$ to fit the position of the peak. The

response as seen in electron scattering is more sensitive to the interior of the nucleus, so we do not expect the same thing in quasielastic nucleon-nucleus scattering. The (p,p') data at lower beam energy and high momentum transfer do show an apparent shift, but we have attributed that to the multiple scattering contributions to the cross section. The residual interactions and also shell structures become more important at smaller momentum transfers. Examples are given in Ref. 5, where the enhancement of the cross section at low excitations due to the isoscalar interaction is shown, and the sensitivity of the peak position in spin-flip reactions to the repulsive interactions in the spin excitation channels is also illustrated.

IV. CONCLUSIONS

Our study of intermediate energy (p,p') reactions on heavy nuclei shows that the main features of the quasielastic peak are quite accurately described by single scattering in the surface response model. The peak position, which is determined by the surface response of semiinfinite nuclear matter in this model, is consistent with the measured spectra. Shell structures become important at small momentum transfers, and they are of course not contained in the semiinfinite model. Single scattering cannot account for the observed spectra at large momentum transfers, in particular at larger energy losses. This

discrepancy is ascribed to multistep processes as indicated by the estimate of double scattering.

The target dependence of the quasielastic peak is determined by Glauber theory for single scattering in the model. The agreement with observed spectra is best for the heaviest targets, and it is surprisingly good even for ^{12}C . This confirms our picture that the quasielastic scattering takes place at the surface of the target nucleus, and that the surface response of heavy nuclei is insensitive to the mass of the target nucleus (except for shell structures).

The comparison at different beam energies shows that the agreement gets better at higher beam energies, for a given energy and momentum transfer. This is consistent with the folding model in which the relative importance of double scattering decreases with increasing beam ener-

gy. Estimates of the effects of Pauli blocking and residual interactions show that medium corrections become important at lower beam energies. The success of the model in explaining the main features of quasielastic, intermediate energy nucleon-nucleus scattering indicates that the quasielastic peak does not contain direct information about the mean free path or other interaction effects in the interior of heavy nuclei.

ACKNOWLEDGMENTS

We are grateful to Ralph E. Segel for providing us with measured proton spectra prior to their publication. This work was supported by the U.S. Department of Energy, Nuclear Physics Division, under Contract W-31-109-ENG-38, and NSF Grant PHY-85-19653.

¹R. E. Segel *et al.* (unpublished).

²J. M. Moss *et al.*, Phys. Rev. Lett. **48**, 789 (1982).

³R. E. Chrien *et al.*, Phys. Rev. C **21**, 1014 (1980).

⁴G. F. Bertsch and O. Scholten, Phys. Rev. C **25**, 804 (1982).

⁵H. Esbensen and G. F. Bertsch, Ann. Phys. (N.Y.) **157**, 255 (1984).

⁶C. Gaarde *et al.*, Nucl. Phys. **A369**, 258 (1981).

⁷F. Osterfeld, D. Cha, and J. Speth, Phys. Rev. C **31**, 372 (1985).

⁸R. E. Segel *et al.*, Phys. Rev. C **32**, 721 (1985).

⁹H. Machner *et al.*, Phys. Lett. **138B**, 39 (1984); J. R. Wu *et al.*, Phys. Rev. C **19**, 698 (1979).

¹⁰H. C. Chiang and J. Huefner, Nucl. Phys. **A349**, 466 (1980).

¹¹H. O. Meyer and P. Schwandt, Phys. Lett. **107B**, 353 (1981).

¹²A. Nadasen *et al.*, Phys. Rev. C **23**, 1023 (1981).

¹³R. Dymarz and T. Kohmura, Phys. Lett. **124B**, 446 (1983).

¹⁴S. Fantoni, B. L. Friman, and V. R. Pandharipande, Phys. Lett. **104B**, 89 (1981).

¹⁵J. W. Negele and K. Yazaki, Phys. Rev. Lett. **47**, 71 (1981).

¹⁶C. W. deJager *et al.*, At. Data Nucl. Data Tables **14**, 479 (1974).

¹⁷R. A. Arndt *et al.*, Phys. Rev. D **28**, 97 (1983).

¹⁸H. Esbensen, H. Toki, and G. F. Bertsch, Phys. Rev. C **31**, 1816 (1985).

¹⁹H. Esbensen and G. F. Bertsch, Phys. Rev. C **32**, 553 (1985).

²⁰J. M. Finn, R. W. Lourie, and B. H. Cottman, Phys. Rev. C **29**, 2230 (1984).